CrossMark

# Transmissible gastroenteritis virus infection induces NF-κB activation through RLR-mediated signaling

Zhen Ding[a,b,1], Kang An[a,b,1], Lilan Xie[c], Wei Wu[a,b], Ruoxi Zhang[a,b], Dang Wang[a,b], Ying Fang[d], Huanchun Chen[a,b], Shaobo Xiao[a,b], Liurong Fang[a,b,*]

[a] State Key Laboratory of Agricultural Microbiology, College of Veterinary Medicine, Huazhong Agricultural University, Wuhan 430070, China
[b] Key Laboratory of Preventive Veterinary Medicine in Hubei Province, the Cooperative Innovation Center for Sustainable Pig Production, Wuhan 430070, China
[c] College of Life Science and Technology, Wuhan Institute of Bioengineering, Wuhan 430415, China
[d] College of Life Sciences, South-Central University for Nationalities, Wuhan 430074, China

ARTICLE INFO

ABSTRACT

Transmissible gastroenteritis virus (TGEV) is a porcine enteric coronavirus which causes lethal severe watery diarrhea in piglets. The pathogenesis of TGEV is strongly associated with inflammation. In this study, we found that TGEV infection activates transcription factors NF-κB, IRF3 and AP-1 in a time- and dose-dependent manner in porcine kidney cells. Treatment with the NF-κB-specific inhibitor BAY11-7082 significantly decreased TGEV-induced proinflammatory cytokine production, but did not affect virus replication. Phosphorylation of NF-κB subunit p65 and proinflammatory cytokine production were greatly decreased after knockdown of retinoic acid-inducible gene I (RIG-I)-like receptors (RLRs) or its adaptors MAVS and STING, while only slight reduction was observed in cells following silencing of Toll-like receptor adaptors, MyD88 and TRIF. Furthermore, TGEV infection significantly upregulated mRNA expression of RIG-I and MDA5. Taken together, our results indicate that the RLR signaling pathway is involved in TGEV-induced inflammatory responses.

## 1. Introduction

Transmissible gastroenteritis virus (TGEV) infection causes severe enteritis accompanied by highly contagious in pigs (Garwes, 1988; Penzes et al., 2001). TGEV is an enveloped, positive-sense, single-stranded RNA virus with a genome of 28.5 kb, belonging to the *Coronaviridae* family in the order *Nidovirales* (Eleouet et al., 1995). The genome consists of a 5' untranslated region (UTR), open reading frame 1a/1b (ORF1a/1b), spike (S), envelope (E), membrane (M), nucleocapsid (N) and 3' UTR, arranged in this order, with three accessory genes 3a, 3b and 7 interspersed within the structural genes at the 3' end of the genome (Putics et al., 2006; Yount et al., 2000). TGEV circulates in pig farms and has been known to mutate, resulting in the S gene deletion mutant now recognized as porcine respiratory coronavirus (PRCV) (Kim et al., 2000; Wang et al., 2010; Wang and Zhang, 2015). It also provides the virus backbone which, in combination with the S gene of porcine epidemic diarrhea virus (PEDV), has generated the recently described chimeric viruses termed swine enteric coronaviruses (SeCoVs) (Belsham et al., 2016). This frequent evolution poses a huge threat to the pig industry.

Virus invasion always triggers an inflammatory response, which is a key mediator of the host response against microbial pathogens (Shrivastava et al., 2016). To monitor and rapidly respond to diverse viruses, germline-encoded pattern recognition receptors (PRRs) are appointed to sense pathogen-associated molecular patterns (PAMPs) and subsequently induce the production of inflammatory mediators with a two-step process: priming and activation (Poeck and Ruland, 2012; Rietdijk et al., 2008). The priming step is mediated primarily by Toll-like receptors (TLRs) or RIG-like receptors (RLRs): TLRs recognize specific viral motifs within the endosomal compartments, then recruit the Toll/IL-1 receptor (TIR) domain-containing adaptors, including myeloid differentiation primary response gene (MyD88) and TIR-domain-containing adaptor-inducing IFN-β (TRIF); RLRs recognize cytosolic viral RNA, then interact with mitochondrial antiviral signaling protein (MAVS, also known as IPS-1/VISA/CARDIF) leading to the recruitment and activation of mitochondria associated complexes (Fukata and Arditi, 2013; Lamkanfi and Dixit, 2009; Takeuchi and Akira, 2010; Tschopp and Schroder, 2010; Yamamoto

---

et al., 2003). In addition, the stimulator of interferon gene (STING, also known as MITA) has also been identified as an adaptor involved in the RLR pathway (Ishikawa and Barber, 2008). The activation step is mainly mediated by cytosolic PRRs including nucleotide binding and oligomerization domain-like receptors (NLRs), absent in melanoma 2 (AIM2), retinoic acid inducible gene I (RIG-I), gamma-interferon-inducible protein 16 (IFI16), and pyrin that initiate assembly of the appropriate inflammasome components where receptors recruit apoptosis-associated speck-like protein containing CARD (ASC) proteins and caspase-1 complexes that are required for the secretion and bioactivity of priming step-produced cytokines (Dutta et al., 2015; Latz et al., 2013; Man et al., 2016; Vajjhala et al., 2014; Yu and Levine, 2011).

The transcription of proinflammatory cytokines are regulated by many transcription factors, including nuclear factor kappa B (NF-κB), activating protein 1 (AP-1), interferon regulatory factor 3 (IRF3) and so on (Hagiwara et al., 2009; Lei et al., 2015; Wang et al., 2008). NF-κB is essential in priming inflammasome activation for production of cytokines like TNF-α, IL-6 and also of pro-IL-1β (Lan et al., 2012; Li and Verma, 2002). The NF-κB family is comprised of five mammalian members: RelA (p65), RelB, cRel, p50 (NF-κB1), and p52 (NF-κB2) (Ghosh et al., 1998). A heterodimer composed of p65 and p50 is the most frequently activated form of NF-κB, interacting with inhibitory kappa B (IκB) molecules in resting cells (Malek et al., 1998). The classical NF-κB activation cascade is initiated by stimulus-induced phosphorylation, ubiquitination and degradation of IκBα, releasing NF-κB dimers and promoting their nuclear translocation. As a result, transcription of various NF-κB target genes involved in the inflammatory response are activated, such as IL-6, IL-8, RANTES and TNF-α (Hayden and Ghosh, 2008).

Previous studies demonstrated that virulent TGEV causes significant inflammation in intestinal tissues, and animal death is mainly attributed to the extreme imbalance of Na+ and K+ ions caused by the severity of the clinical symptoms (Cruz et al., 2013; Saif, 1996). Thus, inflammatory injury to intestinal tissue caused by an overactive immune response is a hallmark of TGEV pathogenesis. Additionally, TGEV-infected cells showed enhanced NF-κB activity and high expression of genes associated with inflammation, including RANTES, CCL2 and CXCL16 (Ma et al., 2014), thus suggesting that the inflammatory response plays an important role in the pathogenicity of TGEV. However, the mechanisms utilized by TGEV to induce NF-κB and inflammatory responses remain largely unknown. In this study, we confirm that TGEV infection enhances NF-κB activation and induces expression of molecules associated with inflammation including IL-6, IL-8, TNF-α and RANTES in porcine kidney (PK)–15 cells. We further analyzed the underlying mechanisms and found that TGEV-activated inflammation mainly depends on the RLR pathway and downstream adaptors MAVS and STING.

## 2. Results

### 2.1. TGEV infection activates NF-κB in PK-15 cells

To explore whether TGEV infection activates NF-κB in PK-15 cells, we first assessed the ability of TGEV to induce NF-κB-dependent promotor activity (NF-κB-Luc) using a luciferase reporter system. To this end, PK-15 cells were transfected with a NF-κB-Luc reporter plasmid and the internal plasmid pRL-TK, followed by infection with TGEV at different multiplicity of infection (MOI). At 24 h post infection (hpi), cells were collected for dual luciferase activity analysis. As shown in Fig. 1A, TGEV infection significantly increased the activity of the NF-κB-dependent promoter in a dose-dependent manner. We also analyzed NF-κB-dependent promotor activity at different time points after TGEV infection (MOI=0.1). Enhanced NF-κB-Luc activity was detected as early as 12 hpi and continued to increase at 24 hpi and 36 hpi (Fig. 1B). However, this activation was not observed in cells treated

with UV-inactivated TGEV (equivalent to 0.1 MOI) (Fig. 1A). These results indicated that TGEV infection could activate NF-κB, and this ability required viral replication. We also tested whether transcription factors IRF3 and AP-1 can be activated after TGEV infection. Similar to NF-κB, TGEV infection activated AP-1 (Fig. 1C) and IRF3 (Fig. 1D) in PK-15 cells.

Activation of NF-κB is usually characterized by degradation of IκBα, phosphorylation of NF-κB subunit p65 and subsequent nuclear translocation (Salminen et al., 2008). Therefore, the expression level of IκBα and phospho-p65 were necessarily detected after TGEV infection in PK-15 cells. At different times postinfection, mock- and TGEV-infected cells were lysed and assayed by immunoblotting using specific antibodies against IκBα, phospho-p65 and total-p65. TNF-α-treated cells were used as a positive control, and PK-15 cells treated with 0.1 MOI UV-inactivated TGEV were used as a negative control. In addition, a specific monoclonal antibody against TGEV N protein was used to monitor viral replication status. As shown in Fig. 2A, the expression of phospho-p65 was increased to 6 fold at 24 hpi in TGEV-infected cells compared with the mock-infected control, and kept 12 fold increase at 36 hpi. Accordingly, TGEV infection induced degradation of IκBα to various degrees throughout the time course, with this being most apparent at 36 hpi. However, UV-inactivated TGEV failed to stimulate IκBα degradation or p65 phosphorylation, indicating that it is not viral particle but live TGEV infection activates NF-κB. Recent study reported the pathogenicity of TGEV is strongly associated with inflammation (Regla-Nava et al., 2015). We compared the ability of virulent and attenuated TGEV to activate NF-κB. PK-15 cells were infected with virulent or attenuated TGEV for 36 h, followed by western blot analysis with antibodies against IκBα, phospho-p65, total-p65. As shown in Fig. 2B, the expression levels of phospho-p65 induced by the attenuated TGEV were significantly low than the virulent TGEV did.

To further determine whether TGEV infection promotes phospho-p65 nuclear translocation, PK-15 cells were transfected with pEGFP-p65, a DNA construct expressing a fusion protein of porcine p65 and green fluorescent protein (GFP). At 24 h post-transfection, the cells were mock-infected or infected with TGEV at 0.1 MOI for 24 h, after which they were fixed and subsequently immunostained with a monoclonal antibody against TGEV N protein and Cy3-conjugated goat anti-mouse IgG. As shown in Fig. 2C, most p65 remained in the cytoplasm in mock-infected cells, while TGEV-infected cells containing the pEGFP-p65 fusion protein showed obvious nuclear accumulation of p65. These data demonstrated that TGEV infection induced phosphorylation and nuclear translocation of p65 and degradation of IκBα.

### 2.2. Effect of NF-κB on TGEV-induced proinflammatory cytokine expression

To further investigate whether TGEV infection induces proinflammatory cytokine production through the NF-κB signaling pathway, the mRNA expression of various proinflammatory cytokines (IL-6, IL-8, TNF-α and RANTES) were detected by quantitative reverse transcription-polymerase chain reaction (qRT-PCR). To this end, PK-15 cells were pretreated with BAY11-7082, a NF-κB-specific inhibitor, at different doses (1, 2, 5, and 10 μM) or left untreated, but subjected to an equal volume of DMSO, for 1 h, followed by inoculation with TGEV (MOI=0.1). All tested doses of BAY11-7082 used in the present study had no detectable cytotoxicity in PK-15 cells, determined by MTT assay (data not shown). After incubation for 1 h, the supernatant was removed and replaced with cell culture media containing different doses of the inhibitor BAY11-7082.RT-qPCR was performed with total RNA collected from different cell samples at 24 hpi. As shown in Fig. 3A, the levels of IL-6, IL-8, TNF-α, and RANTES mRNAs were significantly upregulated in TGEV-infected cells at 24 hpi, compared with the mock-infected group. Furthermore, the effects of TGEV-induced proinflammatory cytokine expression were reduced in a dose-dependent manner after treatment with the NF-κB inhibitor.
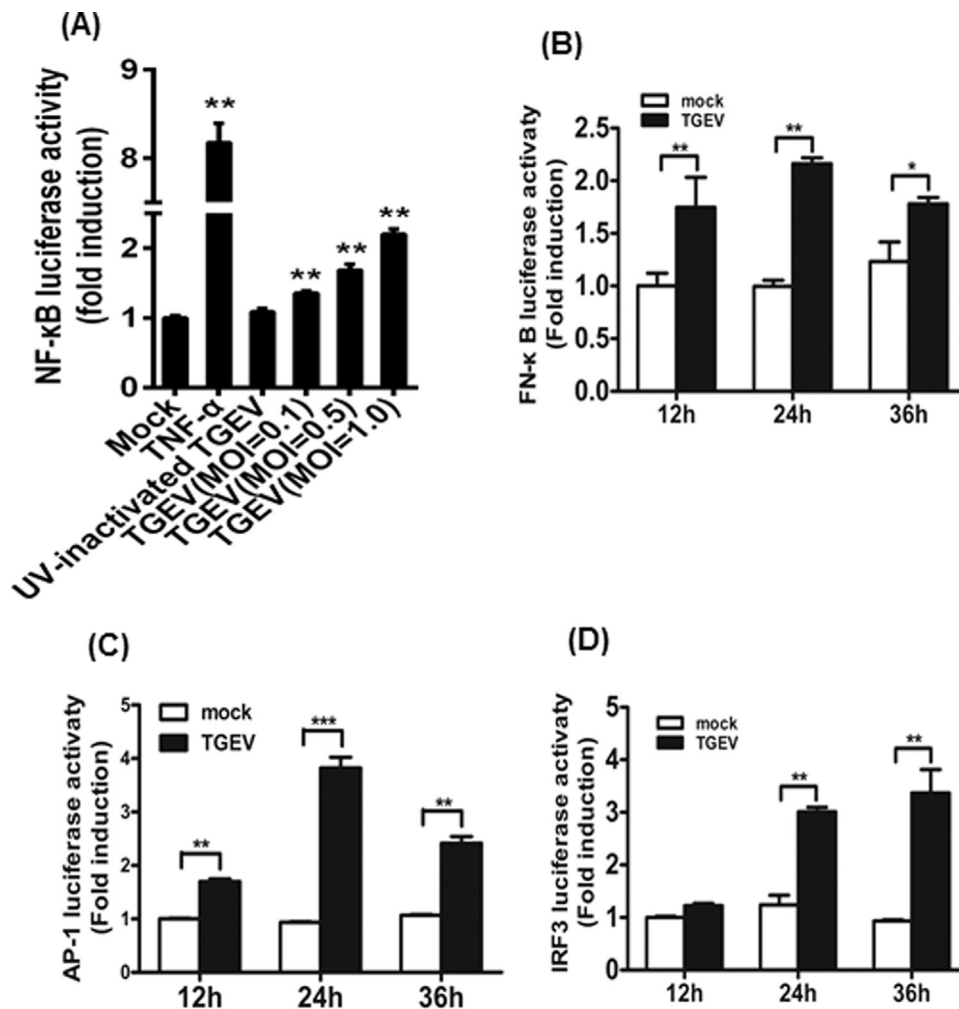
**Fig. 1.** TGEV infection activates NF-κB. (A) PK-15 cells were co-transfected with NF-κB-Luc reporter plasmid (0.2 μg) and pRL-TK plasmid (0.05 μg) for 24 h. Then cells were infected with TGEV (MOI=0.1, 0.5, or 1) or UV-inactivated TGEV for 24 h, or treated with 40 ng/mL TNF-α for 6 h. Cells were then harvested and analyzed for luciferase activity. (B-D) PK-15 cells were co-transfected with NF-κB-Luc (B) or AP-1-Luc (C) or IRF3-Luc (D) reporter plasmids (0.2 μg), together with pRL-TK plasmids (0.05 μg) for 24 h. Then cells were mock infected or infected with 0.1 MOI TGEV. Whole cell lysates were then prepared at 12, 24 or 36 hpi and subjected to luciferase activity analysis. Values are representative of the mean of three independent experiments and error bars represent standard deviations. $^{*}P < 0.05$, $^{**}P < 0.01$ and $^{***}P < 0.001$.

We also determined the virus titers after treatment with BAY11-7082 and found that the inhibitor did not significantly affect virus titers at any recorded timepoint (Fig. 3B), indicating that the effect observed above was due to a decrease in NF-κB activation, rather than the inhibition of viral replication. Taken together, these data demonstrate that NF-κB activation induces the expression of proinflammatory cytokines after TGEV infection.

*2.3. TGEV infection activates NF-κB through the RLR-dependent pathway*

The priming step to activate the production of inflammatory cytokines is mediated primarily by TLRs and/or RLRs signaling (Shrivastava et al., 2016). To determine which signaling pathway is triggered by TGEV to activate NF-κB, specific siRNAs targeting MyD88, TRIF, MAVS, and STING, adaptor molecules in the TLR and RLR pathways, were synthesized. The knockdown efficiency of each siRNA was demonstrated by transient transfection and RT-qPCR assays (Fig. 4A). Cells were transfected with each siRNA followed by TGEV infection. As shown in Fig. 4B, siRNAs targeting MAVS and STING but not MyD88 or TRIF significantly reduced the expression of phospho-p65 in TGEV-infected cells. Densitometric analysis of three independent experiments using gene tools (ImageJ1.44p) also showed that the densitometric ratio of phospho-p65 to p65 was markedly diminished in

cells transfected with siMAVS or siSTING, compared with the control (siCtrl) following TGEV infection. These results further demonstrate that MAVS and STING, rather than MyD88 and TRIF, involved in TGEV-mediated inflammatory responses.

It is well known that MAVS is a major adaptor protein for the viral RNA sensors RIG-I and MDA5, and STING is also associated with MAVS downstream in the RLR pathway (Ishikawa et al., 2009; Zhong et al., 2008). Because knockdown of MAVS or STING impaired TGEV-induced NF-κB activation, it is possible that TGEV-induced NF-κB activation depends on the RLR pathway. To further demonstrate this hypothesis, specific siRNAs targeting RIG-I and MDA5 were designed. The synthesized siRNAs efficiently knocked down the mRNA expression of endogenous RIG-I and MDA5 (Fig. 5A). Similar to results obtained from siRNA targeting MAVS or STING, silencing of RIG-I and MDA5 also reduced expression of phospho-p65 in TGEV-infected cells (Fig. 5B).

*2.4. TGEV infection upregulates RIG-I and MDA-5 mRNA expression*

To determine whether TGEV infection affects the expression of RIG-I and MDA-5, PK-15 cells were infected with 0.1 MOI of TGEV at various time points. Total RNA was isolated and the expression of RIG-I and MDA5 was determined by RT-qPCR. As shown in Fig. 5C, the expression of RIG-I and MDA5 mRNA was upregulated in TGEV-
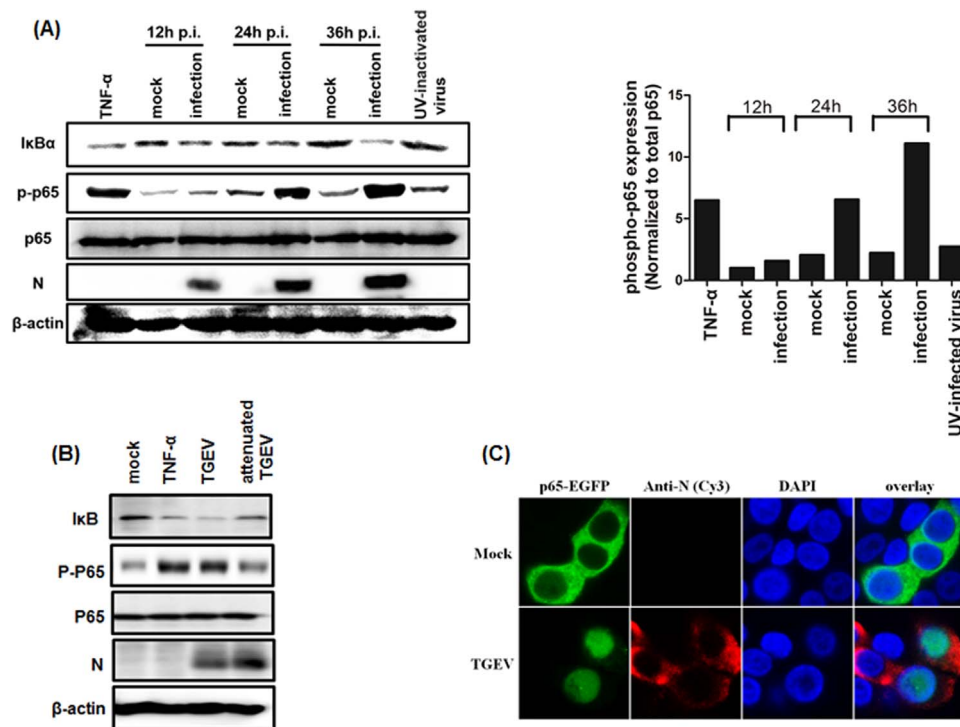
**Fig. 2.** TGEV infection induces degradation of IκBα, phosphorylation and nuclear translocation of p65. (A) PK-15 cells were mock infected or infected with TGEV (MOI=0.1) for 12, 24 or 36 h. Cells infected with an equal amount of UV-inactivated TGEV for 36 h were used as a negative control, and cells stimulated with 40 ng/mL TNF-α for 6 h were set as a positive control. Whole cell lysates were collected and subjected to western blot analysis with antibodies against phosphorylated p65 (p-p65), p65, IκBα, TGEV N protein or β-actin. The ratios of p-p65: total p65 were estimated by densitometry of corresponding bands using gene tools (ImageJ1.44p) and are shown as a bar diagram. (B) PK-15 cells were treated with TNF-α, or infected with virulent TGEV (MOI=0.1) or attenuated TGEV (MOI=0.1) for 36 h. Cells were harvested for western blot analysis with phosphorylated p65 (p-p65), p65, TGEV N protein or β-actin antibodies. (C) PK-15 cells were transfected with 1 μg pEGFP-p65 for 24 h, and then mock-infected or infected with TGEV (MOI=0.1). At 24 hpi, the cells were fixed for immunofluorescence assay to detect TGEV N protein (red). Cellular nuclei were counterstained with DAPI (blue). Fluorescent images were examined under confocal laser scanning microscopy (LSM 510 Meta, Carl Zeiss).

infected cells compared with that observed in mock-infected cells. RIG-I and MDA5 mRNAs were detected as early as 12 hpi and reached a peak at 24 hpi, before declining slightly at 36 hpi. We did not detect the expression of RIG-I or MDA-5 at the protein level because no antibody against porcine RIG-I and MDA-5 is available. These data indicated RIG-I and MDA5 involved in NF-κB signaling activation after TGEV infection.

### 2.5. TGEV infection induces production of proinflammatory cytokines via RLR-mediated signaling

To further determine the effect of RLR-mediated signaling on TGEV-induced proinflammatory cytokine production, we used siRNAs targeting specific adaptors or receptors to interfere in the signaling pathway. PK-15 cells were transfected with specific siRNAs or negative control siRNA, followed by TGEV infection, and the expression of various proinflammatory cytokines were analyzed by RT-qPCR. As shown in Fig. 6, knockdown of RIG-I, MDA5, MAVS or STING significantly decreased TGEV-induced proinflammatory cytokine mRNA expression, including IL-6, IL-8, TNF-α and RANTES. Consistent with the results of the NF-κB activation analysis, no appreciable changes were observed in cells transfected with siRNA targeting MyD88 or TRIF compared with cells transfected with siCtrl. These results further support the conclusion that TGEV infection triggers NF-κB activation via RLR-mediated signaling.
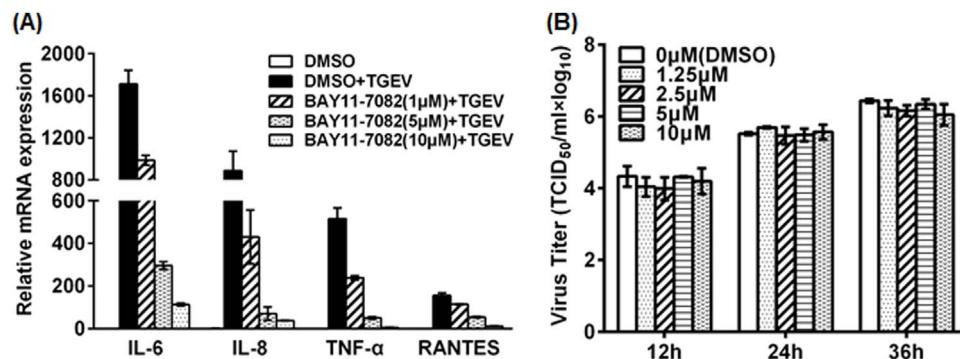


**Fig. 3.** Effect of NF-κB on proinflammatory cytokine induction after TGEV infection. PK-15 cells were pretreated or nontreated (exposed to equal amounts of DMSO) with a specific NF-κB inhibitor BAY11-7082 at different doses (1, 5, and 10 μM) for 1 h, followed by inoculation with TGEV (MOI=0.1) for 1 h. (A) Cells were lysed to extract total RNA, which was used to detect the expression of IL-6, IL-8, TFN-α, RANTES and GAPDH genes by RT-qPCR. (B) The infected cells were collected and virus titers were determined by TCID$_{50}$. Values are presented as the mean ± SD from three independent experiments performed in triplicate.
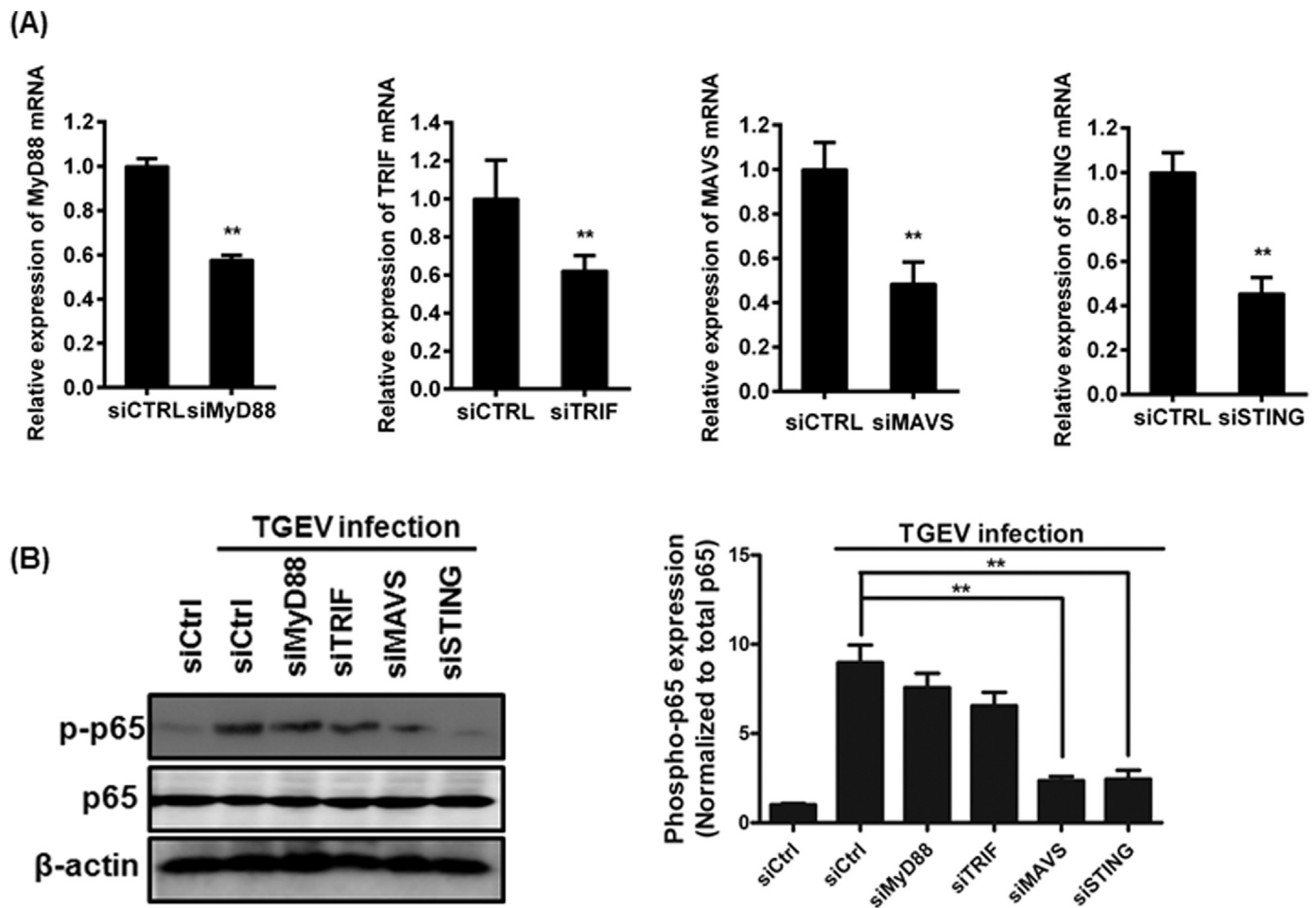
**Fig. 4.** TGEV activates NF-κB through a MAVS- and STING-mediated pathway. (A) SiRNA interference. PK-15 cells were transfected with 50 nM specific siRNA targeting MyD88, TRIF, MAVS or STING, or a negative control siRNA for 24 h, then cells were collected for analysis of MyD88, TRIF, MAVS and STING mRNA levels by using RT-qPCR assays. (B) PK-15 cells were transfected with 50 nM specific siRNA targeting MyD88, TRIF, MAVS or STING, or a negative control siRNA for 24 h and then cells were mock- or TGEV-infected (MOI=0.1). At 24 hpi, cells were harvested and subjected to western blot analysis with specific antibodies against phosphorylated p65 (p-p65), p65 and β-actin. Fold changes in the ratio of p-p65:total p65 were estimated by densitometry of corresponding bands using gene tools (ImageJ1.44p). These data are representative of the results of three independent experiments and error bars represent standard deviations ($^*P < 0.05$ and $^{**}P < 0.01$).

## 3. Discussion

Regulation of NF-κB is an important strategy utilized by viruses for manipulation of the immune response or immune escape. In the case of coronaviruses, previous results have suggested that severe acute respiratory syndrome coronavirus (SARS-CoV) and Middle East respiratory syndrome CoV can escape antiviral innate immunity by impairing NF-κB activation (DeDiego et al., 2014; Matthews et al., 2014). On the contrary, both mouse hepatitis virus (MHV) and PEDV can activate NF-κB signaling mediated by RLRs and TLRs, respectively (Cao et al., 2015; Li et al., 2010). Similar to PEDV and MHV, TGEV infection also activates proinflammatory cytokine expression (Cruz et al., 2013). In the present study, we describe for the first time the underlying mechanisms of NF-κB activation in response to TGEV infection, and identified that this activation was mediated by the RLR pathway.

RIG-I has a highly homologous structure with MDA5, but the virus-derived PAMPs detected by these two sensors are not identical. RIG-I primarily senses vesicular stomatitis virus, influenza virus, hepatitis C virus, and Japanese encephalitis virus (Kato et al., 2008, 2006; Loo et al., 2008; Nakhaei et al., 2009; Sumpter et al., 2005); MDA5 mainly detects picornaviruses and the dsRNA analog polyinosine-polycytidylic aid [poly(I:C)] (Kato et al., 2006; Wies et al., 2013); RIG-I and MDA5 function redundantly in the detection of Dengue virus and West Nile virus as well as paramyxoviruses (Kato et al., 2006; Loo et al., 2008). In

addition, some viruses can up-regulate the expression of RIG-I and MDA5. For example, RIG-I expression levels are rapidly increased upon Sendai virus or influenza virus infection; encephalomyocarditis virus infection or poly(I:C) treatment also increase the expression of MDA5 (Wies et al., 2013). We observed in this study that TGEV infection boosted both RIG-I and MDA5 expression, which indicated that TGEV can be sensed by both RIG-I and MDA5, thus amplifying RLR-mediated proinflammatory cytokines to perpetuate the immuno-pathology progress. RLR inflammasomes regulate RNA virus-induced proinflammatory cytokine production via two mechanisms: (1) RIG-I and MDA5 can recruit MAVS, triggering caspase-8 and Fas-associated death domain protein activated-NF-κB for production of proinflammatory cytokines; (2) RIG-I and MDA5 can also bind ASC and thereby trigger caspase-1-dependent inflammasome activation via a NLRP3-independent mechanism (Loo et al., 2008; Poeck and Ruland, 2012). Further studies are required to define the detailed mechanism(s) involved in TGEV-induced proinflammatory cytokine production.

TGEV is an RNA virus with a large, 28.5 kb genome, with replication intermediates including 5'-triphosphate and certain duplex RNA structures, which are classical ligands sensed by RIG-I and MDA5 (Cui et al., 2008; Faivre et al., 2016; Wu et al., 2013). However, MDA5 seems to have a greater effect than RIG-I on sensing TGEV, since silencing MDA5 more severely impaired NF-κB activation than did knockdown of RIG-I. It is known that RIG-I preferentially recognizes non-self RNA sequences containing 5' triphosphorylated (5'ppp) ends
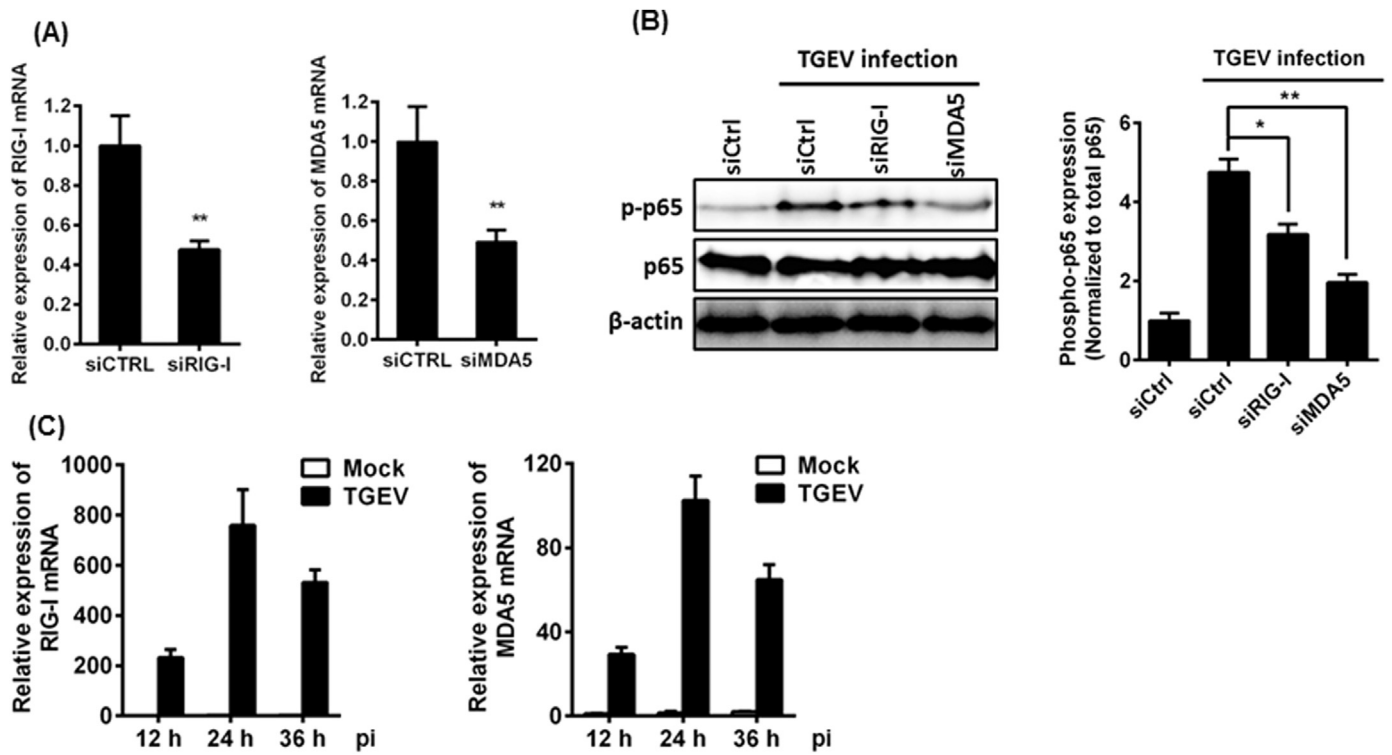
**Fig. 5.** RIG-I and MDA5 are required to activate NF-κB in TGEV-infected cells. (A) SiRNA interference. PK-15 cells were transfected with 50 nM specific siRNAs targeting RIG-I, MDA5 or negative control siRNA for 24 h, then cells were collected for analysis of mRNA levels using RT-qPCR assays. (B) PK-15 cells were transfected with 50 nM specific siRNAs targeting RIG-I, MDA5 or negative control siRNA for 24 h and then cells were mock- or TGEV-infected (MOI=0.1). At 24 hpi, cells were harvested and subjected to western blot analysis with specific antibodies against phosphorylated p65 (p-p65), p65 and β-actin. Fold changes in the ratio of p-p65: total p65 were estimated by densitometry of corresponding bands using gene tools (ImageJ1.44p) and are shown as a bar diagram. (C) PK-15 cells were mock-infected or infected with TGEV (MOI=0.1), and then total RNA was extracted from lysates of the different cell samples at 12, 24 and 36 hpi. The mRNA levels of RIG-I and MDA5 were assessed by RT-qPCR and normalized to that of porcine GAPDH. These data are representative of the results of three independent experiments and error bars represent standard deviations ($^*P < 0.05$ and $^{**}P < 0.01$).
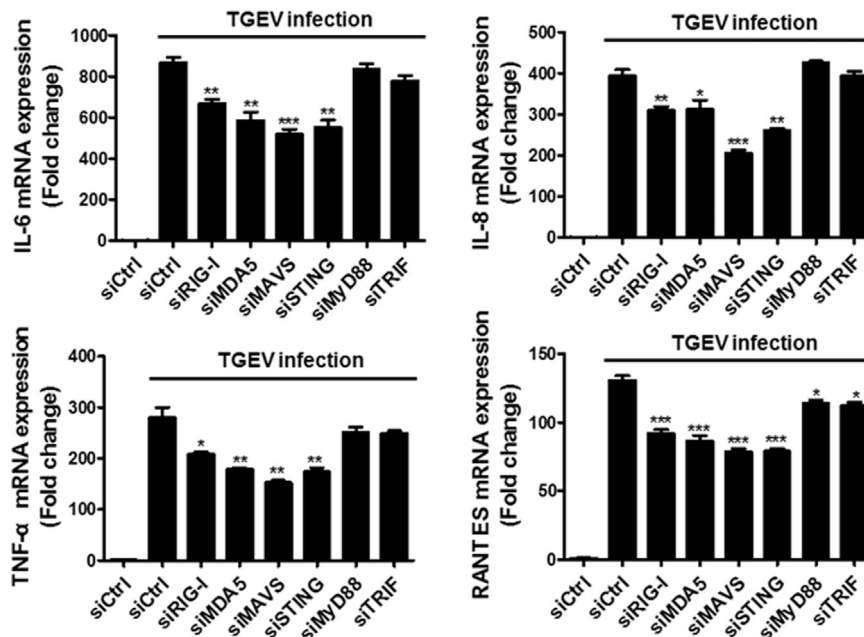


**Fig. 6.** TGEV infection induces production of proinflammatory cytokines via RLR-mediated signaling. PK-15 cells were transfected with 50 nM specific siRNAs targeting various signaling molecules or negative control siRNA for 24 h, and then cells were mock- or TGEV-infected (MOI=0.1). Total RNA was extracted from lysates of the different cell samples at 24 hpi. The mRNA levels of each cytokine gene were assessed by RT-qPCR and normalized to that of porcine GAPDH. These data are representative of the results of three independent experiments and error bars represent standard deviations. $^*P < 0.05$, $^{**}P < 0.01$ and $^{***}P < 0.001$.

or short dsRNA, while MDA5 can bind long dsRNA molecules with blunt ends (Hornung et al., 2006; Kato et al., 2008). Coronaviruses can modify their mRNA 5' structures by encoding several nonstructural proteins (nsp) with RNA capping activity to evade innate immune recognition, such as nsp14 (N7-methyltransferase) and nsp10/16 complex (2'-O-methyltransferase). Therefore, MDA5 is regarded as an important sensor for recognizing coronaviruses.

The inflammatory response is vital for orchestrating the immune

response against pathogens. It has been reported that NF-κB inhibitors may be effective as antiviral agents against influenza virus, functioning mainly by reducing virus titers (Pinto et al., 2011; Wiesener et al., 2011). Intriguingly, treatment with BAY11-7082 had no impact on TGEV replication in PK-15 cells, a phenomenon which has also been described for human coronaviruses infecting the respiratory tract, such as pandemic SARS-CoV (DeDiego et al., 2014). Theoretically, it would be expected that a reduced antiviral response should lead to an increase in viral replication, ultimately resulting in higher virus titers. However, if TGEV-induced inflammatory cytokines could not reach the minimal concentration necessary to affect TGEV replication, it is not surprising that an effect on virus titers was not detectable. TGEV infection also promotes IFN-β production and interferon-stimulated genes (ISGs) expression, but this is much lower than the concentration required to inhibit viral replication (An et al., 2014; Becares et al., 2016; Zhu et al., 2017). However, NF-κB inhibitors remain potential therapeutic drugs against TGEV, being associated with reduced expression of proinflammatory cytokines and alleviated inflammation-induced pathology.

The inflammation triggered by RNA viruses may be caused by two RLR agonists: replication intermediates and virus-encoded proteins, and nucleic acid motifs (Cui et al., 2008; Triantafilou et al., 2012). However, TGEV-encoded protein behavior in inflammation regulation is still unclear. Regarding other coronavirus, the SARS-CoV N protein activates IL-6 expression through NF-κB by facilitating the translocation of NF-κB from the cytosol to the nucleus or by binding directly to the NF-κB element on the promoter (Zhang et al., 2007). The SARS-CoV S protein up-regulates IL-6 and TNF-α expression in murine macrophages, or IL-8 in human peripheral blood monocyte macrophages (Dosch et al., 2009; Wang et al., 2007). The PEDV E protein up-regulates IL-8 expression, which is associated with NF-κB activation (Xu et al., 2013). As for TGEV, protein 7 could reduce inflammatory changes after TGEV infection (Cruz et al., 2013), but no inflammation agonists have been reported. Further study is required to determine whether other TGEV-encoded proteins could regulate inflammation, especially homologs of glycoproteins implicated in other coronaviruses, which are also viral PAMPs and would be detected by PRRs for downstream cascade transduction (Chang et al., 2004; Tang et al., 2012). Defining these issues is important for better understanding of TGEV-induced inflammatory responses.

In conclusion, our data provide an important insight into the pathway involved in TGEV-induced immunopathology. TGEV infection induces proinflammatory cytokine expression, including IL-6, IL-8, TNF-α and RANTES in PK-15 cells, and the RIG-I/MDA5 pathway along with the adapter molecules MAVS and STING play major roles in this process.

## 4. Materials and methods

### 4.1. Cells, virus and reagents

PK-15 cells were grown in Dulbecco's modified Eagle's medium (DMEM) (Invitrogen) supplemented with 10% fetal bovine serum (FBS) (Invitrogen) at 37 °C, 5% $CO_2$. TGEV strain WH-1 (GenBank accession no. HQ462571) was isolated in China, and virus titers were determined by 50% tissue culture infective doses ($TCID_{50}$). For TGEV UV inactivation, 15 mL of virus inoculum was placed into a 10-cm-diameter dish on ice and exposed to UV light of wavelength 254 nm for 30 min. The attenuated TGEV was obtained by continuous passage (97 passages) in PK-15 cells. Polyclonal antibodies against p65, phosphor-p65 and IκBα were purchased from Cell Signaling Technology and the β-actin antibody was purchased from Beyotime (China). The monoclonal antibody against TGEV N protein was made in our laboratory. Horseradish peroxidase-conjugated goat anti-mouse or -rabbit IgGs were purchased from Beyotime (China). The specific NF-κB inhibitor BAY11-7082 was purchased from Sigma and dissolved in DMSO.

### 4.2. Transfection and luciferase reporter assay

PK-15 cells seeded on 24-well plates were co-transfected with 0.2 μg reporter plasmid, NF-κB-Luc, AP-1-Luc or IRF3-Luc, and 0.05 μg pRL-TK, followed by infection with TGEV or treatment with TNF-α (Sigma). Cells were then lysed 12 h later and firefly luciferase and Renilla luciferase activities were determined with the dual-luciferase reporter assay system (Promega) according to the manufacturer's protocol. Data are presented as the relative firefly luciferase activities normalized to the Renilla luciferase activities and are representative of three independently conducted experiments.

### 4.3. Immunofluorescence assay

PK-15 cells seeded on glass coverslips (NEST) in 24-well plates were transfected with 1 μg of pEGFP-p65, a DNA construct expressing a fusion protein of porcine p65 and enhanced green fluorescent protein (EGFP) until the cells reached approximately 70–80% confluence. At 24 hpi, cells were infected with TGEV (MOI=0.1) for 24 h and then fixed with cold 4% paraformaldehyde for 10 min and permeated with 0.1% Triton X-100 for 10 min at room temperature. After three washes with PBS, the cells were sealed with PBS containing 5% bovine serum albumin for 1 h, and then incubated with mouse monoclonal antibody against TGEV N protein (made in our laboratory), followed by Cy3-labeled goat anti-mouse IgG (Sigma). Cells were stained with 0.01% 4', 6'-diamidino-2-phenylindole (DAPI) (Invitrogen) to detect nuclei. Fluorescent images were examined by confocal laser scanning microscopy (LSM 510 Meta, Carl Zeiss).

### 4.4. RNA extraction and RT-qPCR

Total cellular RNA was extracted with TRIzol Reagent (Invitrogen) from TGEV-infected PK-15 cells and an aliquot (1 μg) was reverse transcribed to cDNA using AMV reverse transcriptase (Roche, Basel, Switzerland). The cDNA (1 μl of the 20 μl RT reaction) was then used as the template in a SYBR Green PCR assay (Applied Biosystems). The abundance of the individual mRNA transcript in each sample was assayed three times and normalized to that of the internal control, glyceraldehyde-3-phosphate dehydrogenase (GAPDH) mRNA. Primers used are shown in Table 1.

### 4.5. SiRNA-mediated interference

The siRNA targeting pig RIG-I, MDA5, MAVS, STING, MyD88, TRIF or negative control siRNA were synthesized by GenePharma (Shanghai, China), and the target sequences are listed in Table 2. Transient transfection of siRNA was performed using lipofectamine 2000 (Invitrogen) according to the manufacturer's instructions. The dose of siRNA used for transfection was optimized in preliminary experiments and no appreciable cellular toxicity was observed (data not shown).

### 4.6. Western blot analysis

Briefly, PK-15 cells cultured in 60-mm dishes were transfected with specific siRNA prior to TGEV infection, treated with TNF-α, or infected with virulent /attenuated TGEV (MOI=0.1). Cells were then harvested and lysed with buffer (65 mMTris-HCl [pH 6.8], 4% sodium dodecyl sulfate, 3% DL-dithiothreitol, and 40% glycerol), and protein concentrations were measured in whole cellular extracts. Equal amounts of samples were then subjected to SDS-PAGE and analyzed for expression of TGEV N protein, IκBα, p65 or p-p65 protein by western blotting using the indicated antibodies. Expression of β-actin was detected to demonstrate equal protein sample loading.

**Table 1**
Quantitative reverse transcription PCR primers.

| Gene name | Forward primer sequence (5'–3') | Reverse primer sequence (5'–3') |
|---|---|---|
| GAPDH | ACATGGCCTCCAAGGAGTAAGA | GATCGAGTTGGGGCTGTGACT |
| IL-6 | CTGCTTCTGGTGATGGCTACTG | GGCATCACCTTTGGCATCTT |
| IL-8 | AGTTTTCCTGCTTTCTGCAGCT | TGGCATCGAAGTTCTGCACT |
| RANTES | ACACCCTGCTGTTTTTCCTACCT | AGACGACTGCTGCCATGGA |
| TNF-α | CGTTGTAGCCAATGTCAAAGCC | TGCCCAGATTCAGCAAAGTCCA |
| RIG-I | AGAGCAGCGGCGGAATC | GGCCATGTAGCTCAGGATGAA |
| MDA5 | TCCGGGAAACAGGCAACTC | CAAAGGATGGAGAGGGCAAGT |
| MyD88 | GGCAGCTGGAACAGACCAA | GGTGCCAGGCAGGACATC |
| TRIF | ACTCGGCCTTCACCATCCT | GGCTGCTCATCAGAGACTGGTT |
| MAVS | TGGGTACAGTCCTTCATCGG | GGGTAACTTGGCTCATCCTCT |
| STING | TTACATCGGGTACCTGCGGC | CCGAGTACGTTCTTGTGGCG |

**Table 2**
Short interfering RNA target sequences.

| Gene name | The target sequence (5'–3') |
|---|---|
| RIG-I | CUCUUGGAGGCUUAUUUCA |
| MDA5 | GAGAAACCAGUGAUUCCCU |
| MyD88 | CGGCUGAAGUUAUGUGUGU |
| TRIF | CCACCUUUCAGAAGAAGAU |
| MAVS | CUGCUGCGGAAUUCAAACA |
| STING | CAUUCGCUUCCUGCACGAG |

## 4.7. Statistical analysis

Data are presented as the mean ± SD for at least three independent experiments. Student's *t*-test was used to analyze differences between two experimental groups. A *P*-value less than 0.05, 0.01 and 0.001 were considered significant, highly significant and extremely significant, respectively.

## Acknowledgements

## References

An, K., Fang, L., Luo, R., Wang, D., Xie, L., Yang, J., Chen, H., Xiao, S., 2014. Quantitative proteomic analysis reveals that transmissible gastroenteritis virus activates the JAK-STAT1 signaling pathway. J. Proteome Res. 13, 5376–5390.

Becares, M., Pascual-Iglesias, A., Nogales, A., Sola, I., Enjuanes, L., Zuniga, S., 2016. Mutagenesis of coronavirus nsp14 reveals its potential role in modulation of the innate immune response. J. Virol. 90, 5399–5414.

Belsham, G.J., Rasmussen, T.B., Normann, P., Vaclavek, P., Strandbygaard, B., Botner, A., 2016. Characterization of a novel chimeric swine enteric coronavirus from diseased pigs in Central Eastern Europe in 2016. Transbound. Emerg. Dis. 63, 595–601.

Cao, L., Ge, X., Gao, Y., Ren, Y., Ren, X., Li, G., 2015. Porcine epidemic diarrhea virus infection induces NF-kappaB activation through the TLR2, TLR3, and TLR9 pathways in porcine intestinal epithelial cells. J. Gen. Virol. 96, 1757–1767.

Chang, Y.J., Liu, C.Y., Chiang, B.L., Chao, Y.C., Chen, C.C., 2004. Induction of I L-8 release in lung cells via activator protein-1 by recombinant baculovirus displaying severe acute respiratory syndrome-coronavirus spike proteins: identification of two functional regions. J. Immunol. 173, 7602–7614.

Cruz, J.L., Becares, M., Sola, I., Oliveros, J.C., Enjuanes, L., Zuniga, S., 2013. Alphacoronavirus protein 7 modulates host innate immune response. J. Virol. 87, 9754–9767.

Cui, S., Eisenacher, K., Kirchhofer, A., Brzozka, K., Lammens, A., Lammens, K., Fujita, T., Conzelmann, K.K., Krug, A., Hopfner, K.P., 2008. The C-terminal regulatory domain is the RNA 5'-triphosphate sensor of RIG-I. Mol. Cell 29, 169–179.

DeDiego, M.L., Nieto-Torres, J.L., Regla-Nava, J.A., Jimenez-Guardeno, J.M., Fernandez-Delgado, R., Fett, C., Castano-Rodriguez, C., Perlman, S., Enjuanes, L., 2014. Inhibition of NF-kappaB-mediated inflammation in severe acute respiratory syndrome coronavirus-infected mice increases survival. J. Virol. 88, 913–924.

Dosch, S.F., Mahajan, S.D., Collins, A.R., 2009. SARS coronavirus spike protein-induced innate immune response occurs via activation of the NF-kappaB pathway in human monocyte macrophages in vitro. Virus Res. 142, 19–27.

Dutta, D., Dutta, S., Veettil, M.V., Roy, A., Ansari, M.A., Iqbal, J., Chikoti, L., Kumar, B., Johnson, K.E., Chandran, B., 2015. BRCA1 regulates IFI16 mediated nuclear innate sensing of herpes viral DNA and subsequent induction of the innate inflammasome and interferon-beta responses. PLoS Pathog. 11, e1005030.

Eleouet, J.F., Rasschaert, D., Lambert, P., Levy, L., Vende, P., Laude, H., 1995. Complete sequence (20 kilobases) of the polyprotein-encoding gene 1 of transmissible gastroenteritis virus. Virology 206, 817–822.

Faivre, S., Niccoli, P., Castellano, D., Valle, J.W., Hammel, P., Raoul, J.L., Vinik, A., Van Cutsem, E., Bang, Y.J., Lee, S.H., Borbath, I., Lombard-Bohas, C., Metrakos, P., Smith, D., Chen, J.S., Ruszniewski, P., Seitz, J.F., Patyna, S., Lu, D.R., Ishak, K.J., Raymond, E., 2016. Sunitinib in pancreatic neuroendocrine tumors: updated progression-free survival and final overall survival from a phase III randomized study. Ann. Oncol.. http://dx.doi.org/10.1093/.

Fukata, M., Arditi, M., 2013. The role of pattern recognition receptors in intestinal inflammation. Mucosal Immunol. 6, 451–463.

Garwes, D.J., 1988. Transmissible gastroenteritis. Vet. Rec. 122, 462–463.

Ghosh, S., May, M.J., Kopp, E.B., 1998. NF-kappa B and Rel proteins: evolutionarily conserved mediators of immune responses. Annu. Rev. Immunol. 16, 225–260.

Hagiwara, S., Iwasaka, H., Hidaka, S., Hasegawa, A., Noguchi, T., 2009. Neutrophil elastase inhibitor (sivelestat) reduces the levels of inflammatory mediators by inhibiting NF-kB. Inflamm. Res. 58, 198–203.

Hayden, M.S., Ghosh, S., 2008. Shared principles in NF-kappaB signaling. Cell 132, 344–362.

Hornung, V., Ellegast, J., Kim, S., Brzozka, K., Jung, A., Kato, H., Poeck, H., Akira, S., Conzelmann, K.K., Schlee, M., Endres, S., Hartmann, G., 2006. 5'-Triphosphate RNA is the ligand for RIG-I. Science 314, 994–997.

Ishikawa, H., Barber, G.N., 2008. STING is an endoplasmic reticulum adaptor that facilitates innate immune signalling. Nature 455, 674–678.

Ishikawa, H., Ma, Z., Barber, G.N., 2009. STING regulates intracellular DNA-mediated, type I interferon-dependent innate immunity. Nature 461, 788–792.

Kato, H., Takeuchi, O., Mikamo-Satoh, E., Hirai, R., Kawai, T., Matsushita, K., Hiiragi, A., Dermody, T.S., Fujita, T., Akira, S., 2008. Length-dependent recognition of double-stranded ribonucleic acids by retinoic acid-inducible gene-I and melanoma differentiation-associated gene 5. J. Exp. Med. 205, 1601–1610.

Kato, H., Takeuchi, O., Sato, S., Yoneyama, M., Yamamoto, M., Matsui, K., Uematsu, S., Jung, A., Kawai, T., Ishii, K.J., Yamaguchi, O., Otsu, K., Tsujimura, T., Koh, C.S., Reis e Sousa, C., Matsuura, Y., Fujita, T., Akira, S., 2006. Differential roles of MDA5 and RIG-I helicases in the recognition of RNA viruses. Nature 441, 101–105.

Kim, L., Hayes, J., Lewis, P., Parwani, A.V., Chang, K.O., Saif, L.J., 2000. Molecular characterization and pathogenesis of transmissible gastroenteritis coronavirus (TGEV) and porcine respiratory coronavirus (PRCV) field isolates co-circulating in a swine herd. Arch. Virol. 145, 1133–1147.

Lamkanfi, M., Dixit, V.M., 2009. The inflammasomes. PLoS Pathog. 5, e1000510.

Lan, W., Petznick, A., Heryati, S., Rifada, M., Tong, L., 2012. Nuclear Factor-kappaB: central regulator in ocular surface inflammation and diseases. Ocul. Surf. 10, 137–148.

Latz, E., Xiao, T.S., Stutz, A., 2013. Activation and regulation of the inflammasomes. Nat. Rev. Immunol. 13, 397–411.

Lei, K., Georgiou, E.X., Chen, L., Yulia, A., Sooranna, S.R., Brosens, J.J., Bennett, P.R., Johnson, M.R., 2015. Progesterone and the repression of myometrial inflammation: the roles of MKP-1 and the AP-1 system. Mol. Endocrinol. 29, 1454–1467.

Li, J., Liu, Y., Zhang, X., 2010. Murine coronavirus induces type I interferon in oligodendrocytes through recognition by RIG-I and MDA5. J. Virol. 84, 6472–6482.

Li, Q., Verma, I.M., 2002. NF-kappaB regulation in the immune system. Nat. Rev. Immunol. 2, 725–734.

Loo, Y.M., Fornek, J., Crochet, N., Bajwa, G., Perwitasari, O., Martinez-Sobrido, L., Akira, S., Gill, M.A., Garcia-Sastre, A., Katze, M.G., Gale, M., Jr., 2008. Distinct RIG-I and MDA5 signaling by RNA viruses in innate immunity. J. Virol. 82, 335–345.

Ma, R., Zhang, Y., Liu, H., Ning, P., 2014. Proteome profile of swine testicular cells infected with porcine transmissible gastroenteritis coronavirus. PLoS One 9, e110647.

Malek, S., Huxford, T., Ghosh, G., 1998. Ikappa Balpha functions through direct contacts with the nuclear localization signals and the DNA binding sequences of NF-kappaB. J. Biol. Chem. 273, 25427–25435.

Man, S.M., Karki, R., Kanneganti, T.D., 2016. AIM2 inflammasome in infection, cancer,

and autoimmunity: role in DNA sensing, inflammation, and innate immunity. Eur. J. Immunol. 46, 269–280.

Matthews, K.L., Coleman, C.M., van der Meer, Y., Snijder, E.J., Frieman, M.B., 2014. The ORF4b-encoded accessory proteins of Middle East respiratory syndrome coronavirus and two related bat coronaviruses localize to the nucleus and inhibit innate immune signalling. J. Gen. Virol. 95, 874–882.

Nakhaei, P., Genin, P., Civas, A., Hiscott, J., 2009. RIG-I-like receptors: sensing and responding to RNA virus infection. Semin. Immunol. 21, 215–222.

Penzes, Z., Gonzalez, J.M., Calvo, E., Izeta, A., Smerdou, C., Mendez, A., Sanchez, C.M., Sola, I., Almazan, F., Enjuanes, L., 2001. Complete genome sequence of transmissible gastroenteritis coronavirus PUR46-MAD clone and evolution of the purdue virus cluster. Virus Genes 23, 105–118.

Pinto, R., Herold, S., Cakarova, L., Hoegner, K., Lohmeyer, J., Planz, O., Pleschka, S., 2011. Inhibition of influenza virus-induced NF-kappaB and Raf/MEK/ERK activation can reduce both virus titers and cytokine expression simultaneously in vitro and in vivo. Antivir. Res. 92, 45–56.

Poeck, H., Ruland, J., 2012. From virus to inflammation: mechanisms of RIG-I-induced IL-1beta production. Eur. J. Cell Biol. 91, 59–64.

Putics, A., Gorbalenya, A.E., Ziebuhr, J., 2006. Identification of protease and ADP-ribose 1"-monophosphatase activities associated with transmissible gastroenteritis virus non-structural protein 3. J. Gen. Virol. 87, 651–656.

Regla-Nava, J.A., Nieto-Torres, J.L., Jimenez-Guardeno, J.M., Fernandez-Delgado, R., Fett, C., Castano-Rodriguez, C., Perlman, S., Enjuanes, L., DeDiego, M.L., 2015. Severe acute respiratory syndrome coronaviruses with mutations in the E protein are attenuated and promising vaccine candidates. J. Virol. 89, 3870–3887.

Rietdijk, S.T., Burwell, T., Bertin, J., Coyle, A.J., 2008. Sensing intracellular pathogens-NOD-like receptors. Curr. Opin. Pharmacol. 8, 261–266.

Saif, L.J., 1996. Mucosal immunity: an overview and studies of enteric and respiratory coronavirus infections in a swine model of enteric disease. Vet. Immunol. Immunopathol. 54, 163–169.

Salminen, A., Huuskonen, J., Ojala, J., Kauppinen, A., Kaarniranta, K., Suuronen, T., 2008. Activation of innate immunity system during aging: NF-kB signaling is the molecular culprit of inflamm-aging. Ageing Res. Rev. 7, 83–105.

Shrivastava, G., Leon-Juarez, M., Garcia-Cordero, J., Meza-Sanchez, D.E., Cedillo-Barron, L., 2016. Inflammasomes and its importance in viral infections. Immunol. Res. 64, 1101–1117.

Sumpter, R., Jr., Loo, Y.M., Foy, E., Li, K., Yoneyama, M., Fujita, T., Lemon, S.M., Gale, M., Jr., 2005. Regulating intracellular antiviral defense and permissiveness to hepatitis C virus RNA replication through a cellular RNA helicase, RIG-I. J. Virol. 79, 2689–2699.

Takeuchi, O., Akira, S., 2010. Pattern recognition receptors and inflammation. Cell 140, 805–820.

Tang, D., Kang, R., Coyne, C.B., Zeh, H.J., Lotze, M.T., 2012. PAMPs and DAMPs: signal 0s that spur autophagy and immunity. Immunol. Rev. 249, 158–175.

Triantafilou, K., Vakakis, E., Kar, S., Richer, E., Evans, G.L., Triantafilou, M., 2012. Visualisation of direct interaction of MDA5 and the dsRNA replicative intermediate form of positive strand RNA viruses. J. Cell Sci. 125, 4761–4769.

Tschopp, J., Schroder, K., 2010. NLRP3 inflammasome activation: the convergence of multiple signalling pathways on ROS production? Nat. Rev. Immunol. 10, 210–215.

Vajjhala, P.R., Kaiser, S., Smith, S.J., Ong, Q.R., Soh, S.L., Stacey, K.J., Hill, J.M., 2014. Identification of multifaceted binding modes for pyrin and ASC pyrin domains gives insights into pyrin inflammasome assembly. J. Biol. Chem. 289, 23504–23519.

Wang, C., Chen, J., Shi, H., Qiu, H., Xue, F., Liu, C., Zhu, Y., Liu, S., Almazan, F., Enjuanes, L., Feng, L., 2010. Molecular characterization of a Chinese vaccine strain of transmissible gastroenteritis virus: mutations that may contribute to attenuation. Virus Genes 40, 403–409.

Wang, D., Fang, L., Li, T., Luo, R., Xie, L., Jiang, Y., Chen, H., Xiao, S., 2008. Molecular cloning and functional characterization of porcine IFN-beta promoter stimulator 1 (IPS-1). Vet. Immunol. Immunopathol. 125, 344–353.

Wang, L., Zhang, Y., 2015. Genomic Characterization of a New PRCV Variant,United States, 2014. Transbound. Emerg. Dis. 64, 672–674.

Wang, W., Ye, L., Ye, L., Li, B., Gao, B., Zeng, Y., Kong, L., Fang, X., Zheng, H., Wu, Z., She, Y., 2007. Up-regulation of IL-6 and TNF-alpha induced by SARS-coronavirus spike protein in murine macrophages via NF-kappaB pathway. Virus Res. 128, 1–8.

Wies, E., Wang, M.K., Maharaj, N.P., Chen, K., Zhou, S., Finberg, R.W., Gack, M.U., 2013. Dephosphorylation of the RNA sensors RIG-I and MDA5 by the phosphatase PP1 is essential for innate immune signaling. Immunity 38, 437–449.

Wiesener, N., Zimmer, C., Jarasch-Althof, N., Wutzler, P., Henke, A., 2011. Therapy of experimental influenza virus infection with pyrrolidine dithiocarbamate. Med. Microbiol. Immunol. 200, 115–126.

Wu, B., Peisley, A., Richards, C., Yao, H., Zeng, X., Lin, C., Chu, F., Walz, T., Hur, S., 2013. Structural basis for dsRNA recognition, filament formation, and antiviral signal activation by MDA5. Cell 152, 276–289.

Xu, X., Zhang, H., Zhang, Q., Dong, J., Liang, Y., Huang, Y., Liu, H.J., Tong, D., 2013. Porcine epidemic diarrhea virus E protein causes endoplasmic reticulum stress and up-regulates interleukin-8 expression. Virol. J. 10, 26.

Yamamoto, M., Sato, S., Hemmi, H., Hoshino, K., Kaisho, T., Sanjo, H., Takeuchi, O., Sugiyama, M., Okabe, M., Takeda, K., Akira, S., 2003. Role of adaptor TRIF in the MyD88-independent toll-like receptor signaling pathway. Science 301, 640–643.

Yount, B., Curtis, K.M., Baric, R.S., 2000. Strategy for systematic assembly of large RNA and DNA genomes: transmissible gastroenteritis virus model. J. Virol. 74, 10600–10611.

Yu, M., Levine, S.J., 2011. Toll-like receptor, RIG-I-like receptors and the NLRP3 inflammasome: key modulators of innate immune responses to double-stranded RNA viruses. Cytokine Growth Factor Rev. 22, 63–72.

Zhang, X., Wu, K., Wang, D., Yue, X., Song, D., Zhu, Y., Wu, J., 2007. Nucleocapsid protein of SARS-CoV activates interleukin-6 expression through cellular transcription factor NF-kappaB. Virology 365, 324–335.

Zhong, B., Yang, Y., Li, S., Wang, Y.Y., Li, Y., Diao, F., Lei, C., He, X., Zhang, L., Tien, P., Shu, H.B., 2008. The adaptor protein MITA links virus-sensing receptors to IRF3 transcription factor activation. Immunity 29, 538–550.

Zhu, L., Yang, X., Mou, C., Yang, Q., 2017. Transmissible gastroenteritis virus does not suppress IFN-beta induction but is sensitive to IFN in IPEC-J2 cells. Vet. Microbiol. 199, 128–134.